UDK: 533.6.08(047)
COSATI: 13-01, 20-04

Influence of the Axial Fan Blade Angle on the Turbulent Swirl Flow Characteristics

Đorđe Čantrak[1)]
Novica Janković[1)]
Slavica Ristić[2)]
Dejan Ilić[1)]

The paper presents the investigation of the turbulent swirl flow in a pipe behind the axial fan with adjustable nine blades for the angles of 22°, 26° and 30° for the same rotation number (1500 rpm). Velocities were measured with laser Doppler anemometry (LDA) in the measuring section 3.35·D from the test rig inlet. The achieved Reynolds numbers are Re=236784, 259151 and 277018. The non-homogeneity and anisotropy of the turbulent velocity field are shown. The time averaged circumferential velocity profiles have shown the Rankine vortex structure and revealed a reverse flow in the vortex core region for the blade angles of 26° and 30°. The experimentally determined moments of the second and higher orders reveal complex mechanisms in the turbulent swirl flow. In addition, the visualization of the turbulent swirl flow for an angle of 22° is presented

Key words: **axial fan, turbulence, swirl flow, flow visualization, laser Doppler anemometry.**

Introduction

A turbulent swirl flow generated by an axial fan with three blade angles of $\beta_R = 22^o$ 26° and 30° has been studied in this paper. This complex flow, generated by axial fans, was investigated by various experimental techniques, such as classical probes, hot-wire anemometry, laser Doppler anemometry (LDA) and lately with stereo particle image velocimetry (SPIV) [1-13]. The turbulence structure and a secondary flows analysis on the axial fan pressure side with a variable pitch angle has been studied with the use of a triple HWA probe in [14]. An unsteady flow in axial fans with circumferential skewed blades was studied using a hot-wire anemometry in [15]. Here are also referenced studies of a turbulent swirl flow in a pipe and a diffuser [16-20]. Complex mechanisms of the turbulent swirl flow are studied in [1,3,4,7,16,18,21]. In this paper, a laser Doppler anemometer (LDA) was employed in one measuring section for subsequent measurements of all three velocities: axial (U), radial (V) and circumferential (W). On the basis of the obtained results, the integral characteristics of the turbulent swirl flow were calculated: volume flow rate (Q), averaged axial velocity (U_m), swirl flow number (Ω) and Reynolds number (Re). The non-homogeneity and anisotropy of the turbulent velocity field are also shown.

This paper presents the research of the turbulent swirl flow for three different blade angles (22°, 26° and 30°) and a unique rotation number n = 1500 rpm. Therefore, three Reynolds numbers have been generated. The time averaged velocity profiles have shown the Rankine vortex structure and discovered a reverse flow in the case of the blade angles of 26° and 30°. In addition, the presence of the radial velocity in the vortex core region is shown. The experimentally determined moments of the second and higher orders reveal complex mechanisms in the turbulent swirl flow. It is of interest, from a scientific and engineering point of view, to determine how the blade angle variation affects the integral and statistical characteristics of turbulence. In addition, a visualization technique has been applied for flow visualization.

Experimental test rig and LDA measurements

The experimental test rig for turbulent swirl flow investigation behind the axial fan impeller in a straight pipe is shown in Fig.1. The total length of the experimental test rig is L=27.74·D, where D=0.4 m is an average inner pipe diameter. The position of the measuring section in a transparent pipe, with a wall thickness of 5 mm, measured from the test rig inlet, is x/D=3.35.

Experimental test rig

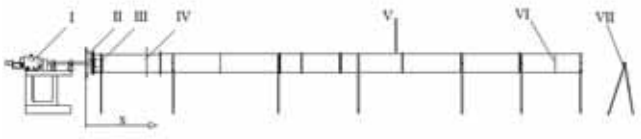

Figure 1. Experimental test rig: I - DC motor 5kW, II - profiled free bell-mouth inlet, III - axial fan (swirl generator), IV - LDA measuring section, V - position of the fog generator probe, VI - flow visualization section and VII - digital camera for visualization.

[1)] Univeristy of Belgrade, Faculty of Mechanical Engineering, Hydraulic Machinery and Energy Systems, Kraljice Marije 16, 11120 Belgrade 35, SERBIA
[2)] Institute Goša, Milana Rakića 35, 11000 Belgrade, SERBIA

The axial fan impeller ZP (Fig.2.a) has an outer diameter D_a=0.399 m, non-dimensional radius D_i/D_a=0.5, where D_i is a hub radius. The fan has nine adjustable blades (Fig.2.b). The blade angle at the diameter D_a was positioned to values β_R=22°, 26° and 30°. These values occur in technical practice. This fan was designed to operate with stay guide vanes and a maximum clearance of 0.5 mm. In this case, the impeller was working without the guide vanes due to a studied problem and a higher clearance value.

a)

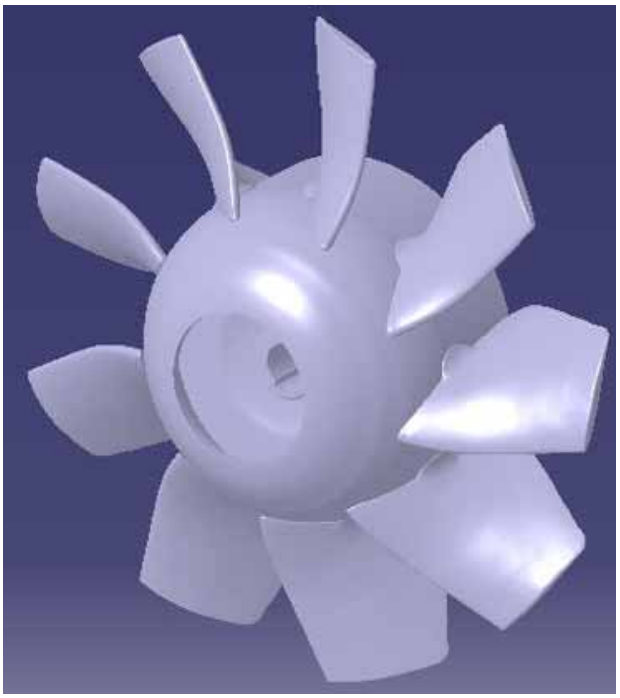

b)

Figure 2. a) Mounted ZP impeller: 1 - profiled inlet and 2 - ZP impeller and b) Scanned and modeled axial fan ZP impeller

The fan rotation speed was regulated by a fully automated thyristor bridge with an error up to ±0.5 rpm. The fan rotational speed of n=1500 rpm is presented here. The ambient conditions have been also recorded.

Fluid flow visualization

Fluid flow visualization was performed in the pipe cross-section and in the vertical meridian plane in the section x/D=26.31. The flow was illuminated with the Nd:Yag laser, New Wave Research, Solo PIV, max power 30 mJ/pulse, wave length 532 nm and frequency 15 Hz. It was operating at 14.5 Hz with an attached cylindrical lens of a focal length of 25 mm and a spherical lens with a focal length of 500 mm. The fog generator probe has approximate Pitot tube geometry and is a part of the smoke generator system (Elven, Precision Limited). The probe has a heater in the head and was operated with the paraffin oil dosed by a precise pump. It was installed at the position x/D=17.24. A digital camera SONY, model DSC-H3, with 10x max optical zoom, F/3.5-4.4, max resolution of 8.1MP and with max 30 fps was used in the movie mode.

LDA measurements

The LDA measurements were performed with a one-component LDA system - Flow Explorer Mini LDA, Dantec with the BSA F30 signal processor unit. The focal length is 285 mm, the laser power is 35 mW and the wavelength is 660 nm. It works in the backscatter mode. The velocity measuring uncertainty was around 0.1%. All three velocities were measured subsequently along the vertical diameter at the points at 10 mm each. Only points with small validation and sampling rate are omitted in the presented diagrams. A recording time of 10 s was set up as the stop criterion for measurements. The flow was seeded by the Antari Z3000II thermal fog machine with liquid EFOG Density Fluid, Invision. The axial fan sucked in the fog.

Application of laser anemometry through curved transparent walls in air flows is a special challenge and demands adequate corrections. Data sampling rates varied along the diameter depending also on the measured velocities. Complex analyses of measurement error, source and level of measurement uncertainty for LDA measurements in this case have been performed in [22,23]. Corrections of the measurement volume position for all three velocities are calculated.

There is also a problem here of the non-uniform particle concentration and spatial variation of particle concentration. The particle motion in the centrifugal field is dominant [24]. Data acquisition and a part of processing were performed in the BSA software.

Results and Analysis

It is of interest, from both a scientific and engineering point of view, to determine how the blade angle affects the integral and turbulence statistical characteristics of the turbulent swirl flow.

Time-averaged velocity fields

The distributions of all three time-averaged velocities, axial (U), circumferential (W) and radial (V) for three various blade angles (β_R=22°, 26° and 30°) are presented in Fig.3. The angle φ=90º denotes the upper part (above-pipe axis) of the vertical diameter, while φ=270º denotes the lower part (under-pipe axis). Velocity distributions are axisymmetrical and have almost the same character for all three blade angles. Circumferential velocity is measured from above and under the pipe due to the focal length. Overlapping of these measured values is in the vortex core and the shear layer.

Circumferential velocity (W) profiles for all three blade angles are similar to the model of the solid body-potential

swirl, i.e. Rankine vortex (Fig.3.c). Four distinct regions are obvious for all three blade angles. Circumferential velocity has almost a linear distribution in the vortex core region, the maximum value in the shear layer, which is followed with the main sound flow region (free vortex) and potential swirl. The last one is the boundary layer region, which was not captured during these measurements. The circumferential velocity maximum values (W_{max}) are the highest for the angle β_R=30° in the point r/R=0.25. The maximum values for other two angles are reached in approximately the same point (r/R=0.2).

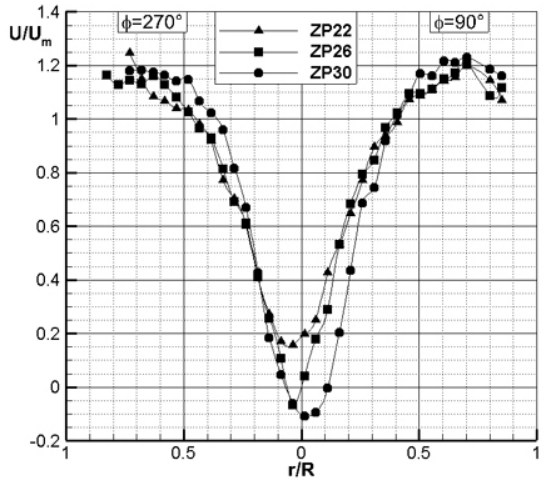

a)

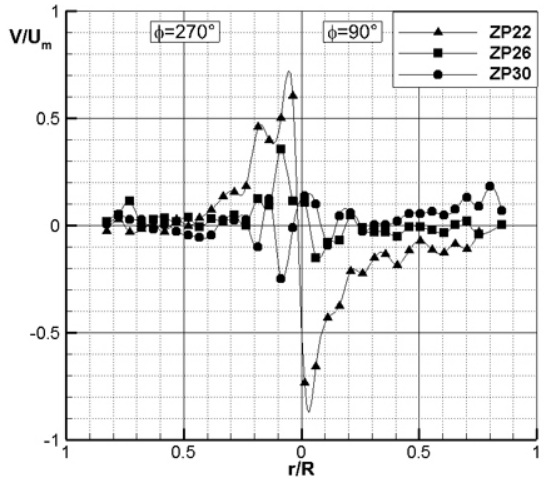

b)

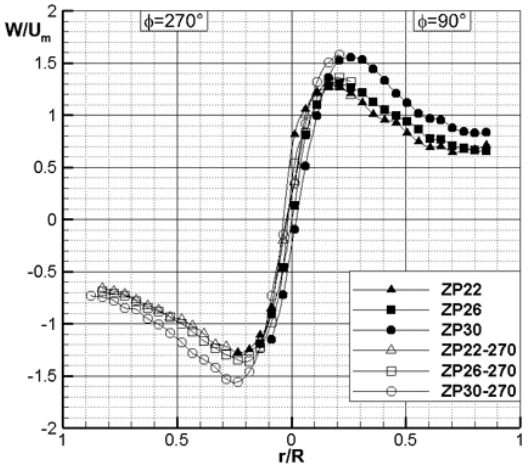

c)

Figure 3. Distributions of the time averaged non-dimensional velocities for all three blade angles in the measuring section: a) axial (U), b) radial (V) and c) circumferential (W)

Circumferential velocity strongly influences distributions of the axial and radial velocities. A reverse flow, i.e. recirculation flow, in the vortex core region is obvious on the non-dimensional axial velocity profiles for the angles β_R = 26° and 30° (Fig.3.a). Axial velocity is almost constant in the main flow region and has the highest values for the β_R=30°.

The highest radial velocities are achieved in the vortex core region and here, the highest radial velocity is for the blade angle β_R=22°, while the lowest one is for the angle β_R=30°. In other fluid flow regions, radial velocity has significantly smaller intensity (Fig.3.b).

On the basis of the axial velocity distribution, volume flow rate (Q) is calculated as well as the averaged axial velocity in volume (U_m) as follows

$$Q = 2\pi R^2 \int_0^1 kU\, dk, \quad U_m = \frac{Q}{R^2\pi}, \tag{1}$$

where k is the dimensionless radius. The Reynolds number is calculated as Re = $U_m D/\nu$, where (ν) is kinematic viscosity.

Average circulation in the measuring section is calculated as follows

$$\Gamma = \frac{4\pi^2 R^3}{Q} \int_0^1 k^2 UW dk. \tag{2}$$

The swirl number is defined as $\Omega = Q/(R\Gamma)$. The integral parameters calculated for all three blade angles are presented in Table 1.

Table 1. Integral parameters for the blade angles β_R = 22°, 26° and 30°.

Angle β_R [°]	Integral parameters				
	Q [m^3/s]	U_m [m/s]	Re	Γ [m^2/s]	Ω
22	1.137	8.83	236784	5.27	1.07
26	1.215	9.43	259151	5.83	1.03
30	1.305	10.13	277018	7.91	0.81

It is obvious that all integral parameters, except for the swirl number, have increased with the blade angle increase (Table 1). The distinction in the swirl number reveals non-similarity among velocity profiles for various blade angles.

Turbulence statistics

Turbulence intensities in axial σ_u, radial σ_v and circumferential σ_w directions are defined as follows

$$\sigma_u = \left(\overline{u^2}\right)^{1/2} = \left[\frac{1}{T}\int_0^T u^2 dt\right]^{1/2}, \quad \sigma_v = \left(\overline{v^2}\right)^{1/2}, \ \sigma_w = \left(\overline{w^2}\right)^{1/2}. \tag{3}$$

In Fig.4, the distributions of the measured turbulence levels σ_i/U_m, , where i=u,v,w for three blade angles, β_R = 22º, 26º and 30º, are presented. It can be noticed that σ_u, σ_v and σ_w, as well as appropriate turbulence levels, σ_i/U_m, i.e. turbulence intensities σ_i normalized by appropriate velocity U_m, reach their highest values in the vortex core and the shear layer region, while in the sound flow region they have significantly lower values. The lowest turbulence levels are reached for angle β_R = 30º and the highest ones for angle β_R = 22º for all flow regions and velocities. The influence of the angle β_R is dominant in the main flow region.

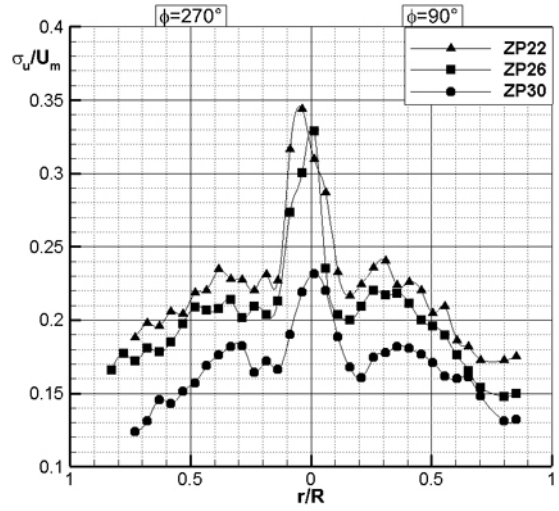

a)

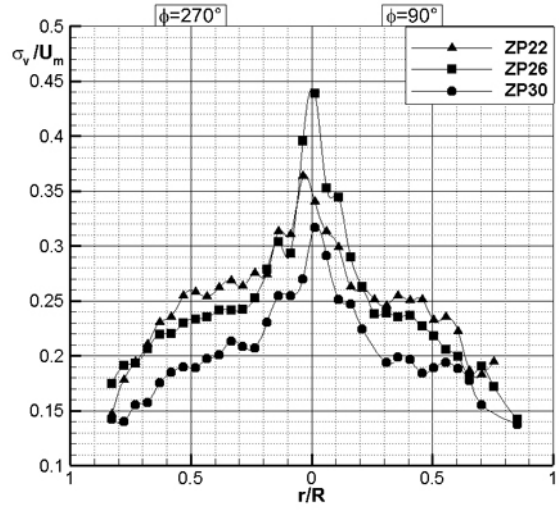

b)

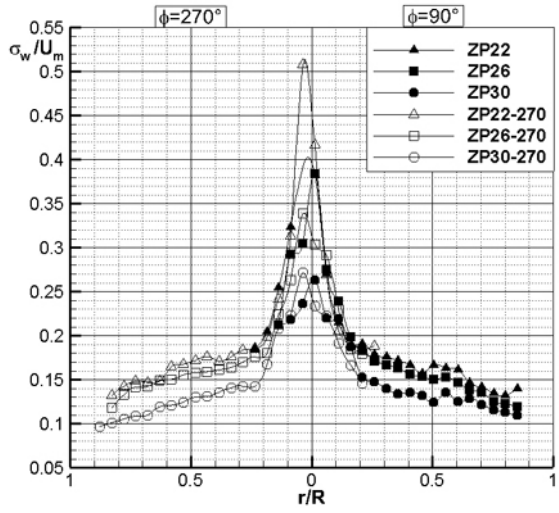

c)

Figure 4. Turbulence levels for three blade angles for the fan ZP: a) axial, b) radial and c) circumferential velocity

The turbulence intensities for all three velocities and for two blade angles β_R=22° (Fig.5.a) and β_R=26° (Fig.5.b) are presented in Fig.5. The character is similar for both blade angles and all velocity components. Maxima for all velocities and both blade angles are reached in the vortex core region. Anisotropy occurs in all flow regions for both blade angles.

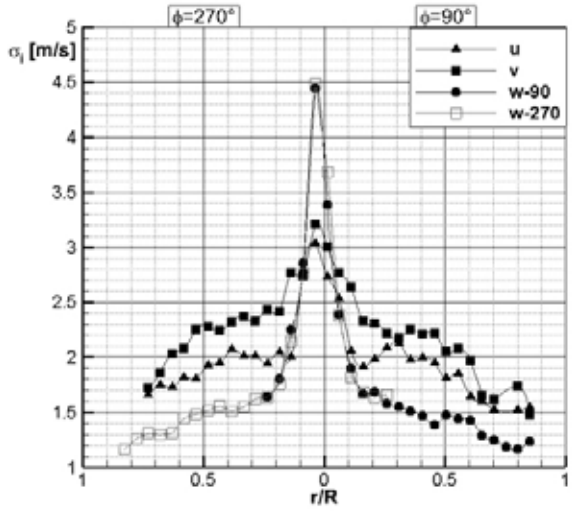

a)

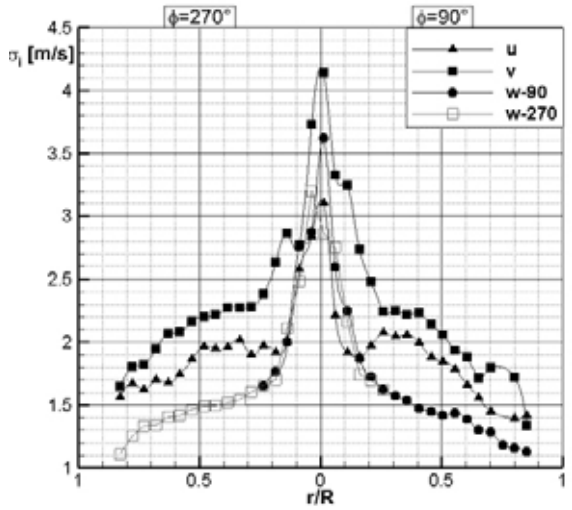

b)

Figure 5. Turbulence intensities for all velocities for angles β_R: a) 22° and b) 26°

The normalized values of the moments of the third order are defined as follows

$$S_u = \overline{u^3}/\sigma_u^3,\ S_v = \overline{v^3}/\sigma_v^3,\ S_w = \overline{w^3}/\sigma_w^3 \qquad (4)$$

and they represent the skewness factors of axial u, radial v and circumferential w fluctuating velocities. The distributions of the skewness factors for all three velocities and three blade angles of the fan ZP are presented in Fig.6. The skewness factors for all three velocities differ from the value for normal, Gaussian distribution (S_u=S_v=S_w=0).

All distributions are non-uniform. The impact of a blade angle is strong on the value and the sign of S_i. The influence of β_R on S_i is expressed in various ways in different zones. For example, β_R acts in different ways in the domains of vortex core and the sound flow region on S_u trends. The biggest positive values $S_{w,max}$≈0.7, obtained for β_R = 22° and 26°, are in the core (Fig.6.c), and the minimum value is S_v≈-1.7, also achieved in the vortex core (Fig.6.b). The skewness factor S_u has the narrowest interval of values -0.6≤ S_u ≤0.25, and, contrary to S_v and S_w, is negative in the vortex core for all values of β_R, except in a small central domain for β_R = 30º. A statistical presentation is clearer if the central moments of the fourth order are also treated, the normalized values F_i of which are calculated as follows

$$F_u = \overline{u^4}/\sigma_u^4,\ F_v = \overline{v^4}/\sigma_v^4,\ F_w = \overline{w^4}/\sigma_w^4. \qquad (5)$$

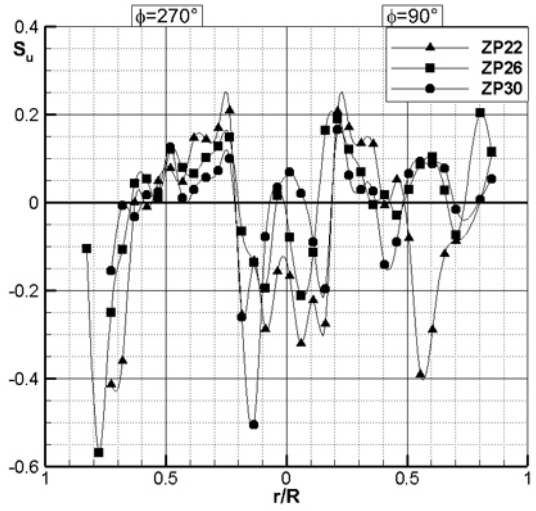

a)

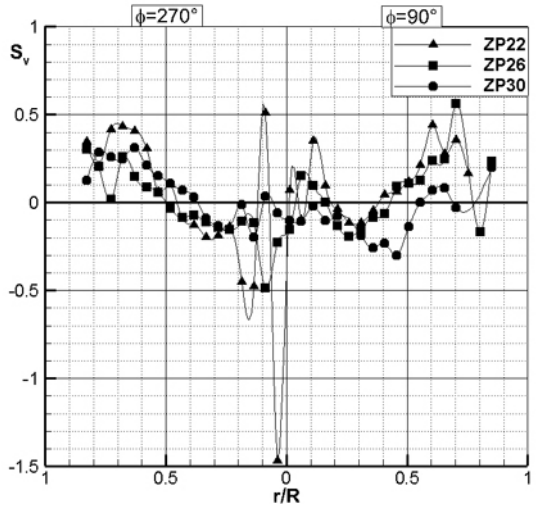

b)

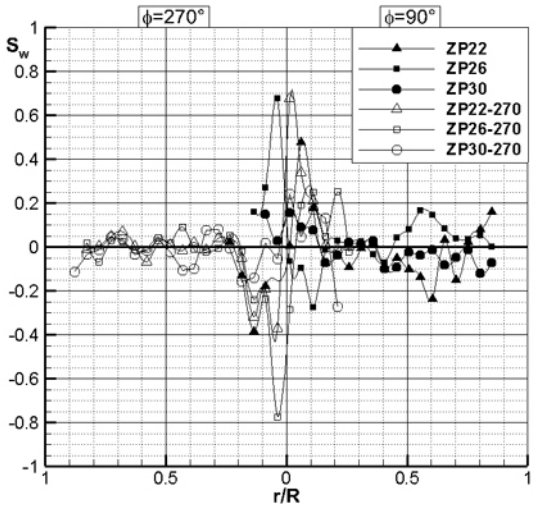

c)

Figure 6. Skewness factor for all three blade angles of the fan ZP: a) axial, b) radial and c) circumferential velocity

All values F_i, i=u,v,w differ from the values for normalized distribution (F_u=F_v=F_w=3). The zones with extreme peaks point out to the presence of small fluctuations which are formed by turbulent eddies motion in the field of small velocity gradients. The influence of the parameter β_R on all three non-uniform distributions F_i is obvious. The values F_v for β_R = 30º are greater than the ones for β_R = 22º (Fig.7.b). The values of F_w in the vortex core region (Fig.7.c) show that it incroporates a wide spectrum of fluctuating circumferential velocities and the motion of turbulence structures of various scales.

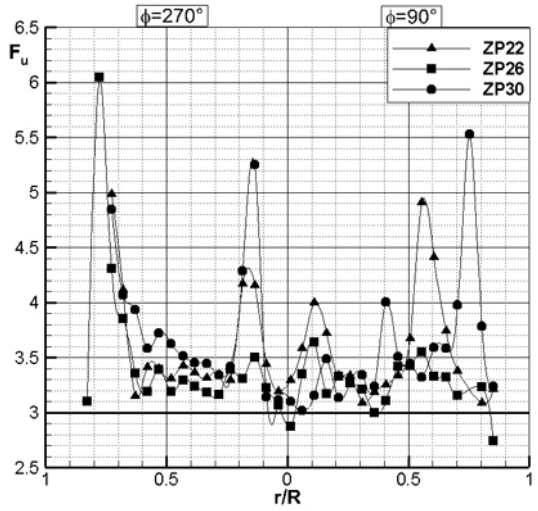

a)

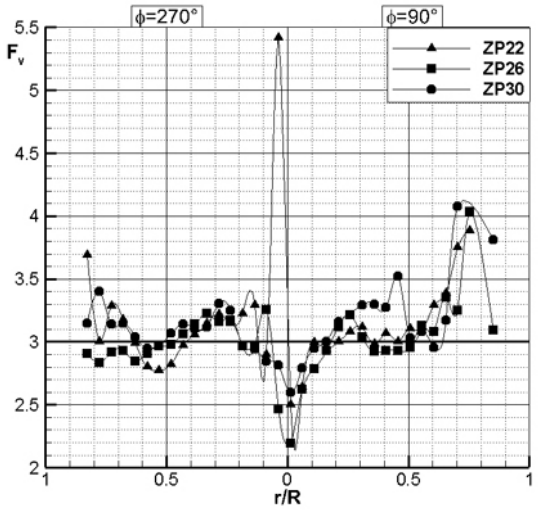

b)

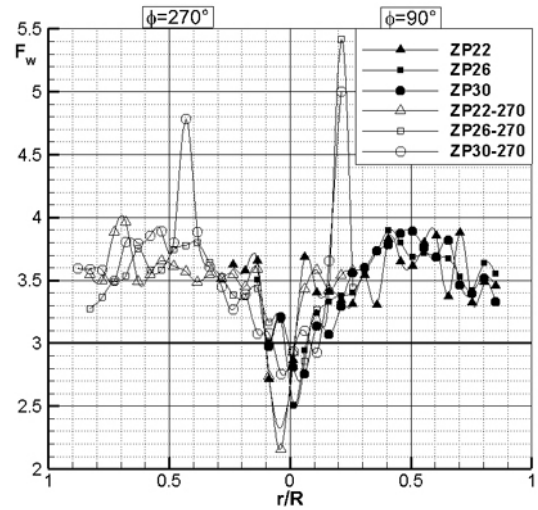

c)

Figure 7. Flatness factor for all three blade angles of the fan ZP for the regime n_3 in the measuring section 1 for: a) axial, b) radial and c) circumferential velocity

Visualization

Turbulent swirl flow visualization has been performed with a specified camera only for an angle of 22° in the specified position in the pipe cross-section (Fig.8.a) and the vertical meridian plane (Fig.8.b).

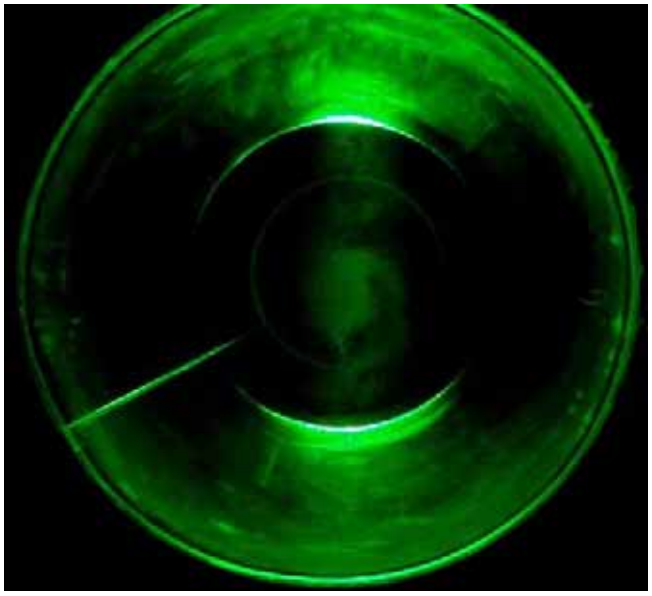

a)

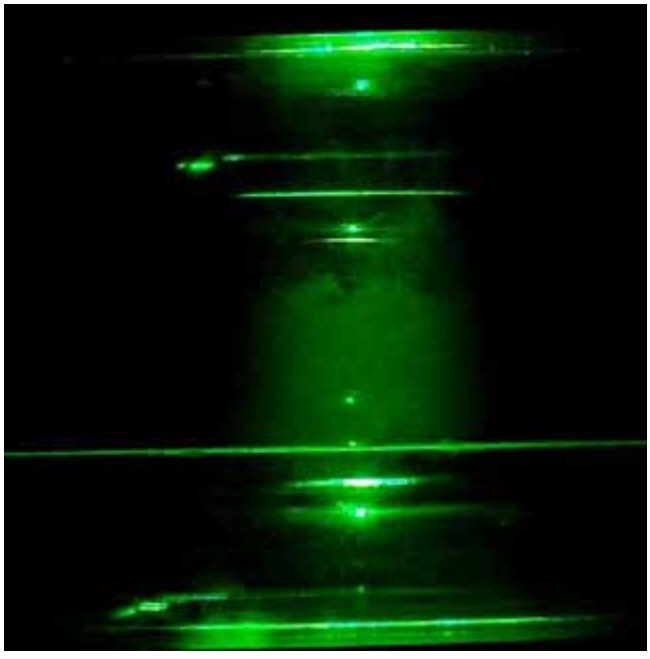

b)

Figure 8. Fluid flow visualization in the: a) cross-section and b) vertical meridian plane.

There is a significant amount of seeding in the vortex core region which is expected due to the velocity and, consequently, the pressure field distribution. This was also shown for ZP22 and the rotation number n = 1000 rpm [25].

Conclusions

Turbulent swirl flow is widely present in nature and technology, and its research has great both theoretical and practical significance. The performed LDA measurements have shown a very good interpretation of turbulent swirl flow measurements. The analysis of the integral and turbulent characteristics of the turbulent swirl flow behind the axial fan impeller has revealed its complexity. The circumferential time averaged velocity profiles have shown the Rankine vortex structure for all three blade angles, while the axial velocity profiles discovered the reverse flow in the vortex core region for the blade angles of 26° and 30°.

The measurements have also shown finite values of radial velocity in the vortex core, with small intensities in all other fluid flow regions. This turbulent field is strongly non-homogeneous and anisotropic. The highest turbulence levels are achieved in the vortex core region for all three blade angles. These flows with high turbulence levels are still undesirable for mathematical modeling, and this type of flow still remains unresolved. It is shown that the turbulence levels for all three velocities reach their maxima in the vortex core region and increase with a swirl number increase, and blade angle decrease.

High values of the measured skewness and flatness factors are characteristic for this flow. They differ from the values for the normalized distribution. This determines a strong asymmetry in the distribution of the probability density of fluctuating velocities, as well the presence of intermittent phenomena in complex processes of turbulent exchange in the turbulent swirl flow. This research will be continued for a range of Reynolds numbers and other fan types.

Acknowledgment

Prof. Dr.-Eng. Zoran Protić† (1922-2010) designed the axial fan impeller which was used in this research. Prof. Zoran Stojiljković, PhD, designed a very precise original fan rotation speed regulator which was used here. This research was financially supported by the Ministry of Education, Science and Technological Development, Republic of Serbia, Project No TR 35046 (2011.-2015.), what is gratefully acknowledged.

References

[1] ČANTRAK,Đ.: *Analysis of the vortex core and turbulence structure behind axial fans in a straight pipe using PIV, LDA and HWA methods*, Ph.D. thesis, Univ. of Belgrade, Faculty of Mech. Eng., Belgrade, 2012.

[2] BENIŠEK,M.: *Investigation of the turbulent swirling flows in straight pipes*, Ph.D. thesis, University of Belgrade, Faculty of Mech. Eng., Belgrade, 1979.

[3] LEČIĆ,M.: *Theoretical and experimental investigations of the turbulent swirling flows*, Ph.D. thesis, Uni. of Belg., Fac. of Mech. Eng., Belgrade, 2003.

[4] ĆOĆIĆ,A.: *Modeling and numerical simulations of swirling flows*, Ph.D. thesis, University of Belgrade, Faculty of Mechanical Engineering, Belgrade, 2013.

[5] MATTERN,P., SIEBER,S., ČANTRAK,Đ., FRÖHLIG,F., CAGLAR,S., GABI,M.: *Investigations on the swirl flow caused by an axial fan: A contribution to the revision of ISO 5801*, Fan 2012, International Conference on Fan Noise, Technology and Numerical Methods, Senlis, France, 18-20.04.2012, CD Proc., 11 pages, fan2012-68-MATTERN.

[6] ČANTRAK,Đ., NEDELJKOVIĆ,M., JANKOVIĆ,N.: *Turbulent swirl flow characteristics and vortex core dynamics behind axial fan in a circular pipe*, Proceedings, Conference on Modelling Fluid Flow (CMFF'12), The 15th International Conference on Fluid Flow Technologies, Budapest, September 4-7. 2012, Vol. II, pp. 749-756.

[7] ČANTRAK,Đ., GABI,M., JANKOVIĆ,N., ČANTRAKS.: *Investigation of structure and non-gradient turbulent transfer in swirling flows*, PAMM, 2012, 12, pp.497-498.

[8] ČANTRAK,Đ., JANKOVIĆ,N.: *Reynolds number influence on the statistical characteristics of turbulent swirl flow*, 4th International Congress of Serbian Society of Mechanics, Vrnjačka Banja, Serbia, 4-7 June 2013, Proceedings, pp. 273-278.

[9] PROTIĆ,Z., NEDELJKOVIĆ,M., ČANTRAK,Đ., JANKOVIĆ,N.: *Novel methods for axial fan impeller geometry analysis and experimental investigations of the generated swirl turbulent flow*, Thermal Science, 2010, 14, pp.S125-S139.

[10] STEENBERGEN,W., VOSKAMP,J.: *The rate of decay of swirl in turbulent pipe flow*, Flow Measurement and Instrumentation, 1998, 9, pp. 67-78.

[11] SIEBER,S., MATTERN,P., CAGLAR,S., GABI,M.: *Time resolved investigation on the swirl flow in the wake of a ducted fan using high speed stereo PIV*, Conference "Laser Methods in Flow Measurements", 4-6. September 2012, Rostock.

[12] RISTIĆ,S.: *Laser Doppler Anemometry and its Application in Wind Tunnel Tests*, Scientific Technical Review, ISSN 1820-0206, 2007, Vol.57, No.3-4, pp.63-75.

[13] LEČIĆ,M.R., ĆOĆIĆ,A.S., ČANTRAK,S.M.: *Original Measuring and Calibration Equipment for Investigation of Turbulent Swirling Flow in Circular Pipe*, Experimental Techniques, 2014, Vol.38, No.3, pp.54-62.

[14] ORO,J.M.F., BALLESTEROS-TAJADURA,R., MARIGORTA,E.B., DÍAZ,K.M.A., MORROS,C.S.: *Turbulence and secondary flows in an axial flow fan with variable pitch blades*, Journal of Fluids Engineering, 2008, 130, pp.041101-1-11.

[15] GUANGYUAN,J., OUAYANG,H., ZHAOHUI,D.: *Experimental investigation of unsteady flow in axial skewed fans according to flow rates*, Experimental Thermal and Fluid Science, 2013, 40, pp. 81-96.

[16] ČANTRAK,S.: *Experimental investigation of statistical properties of turbulent swirl flow in pipe and diffusers*, Ph.D. thesis, Karlsruhe University (TH), Institute of Fluid Machinery, 1981.

[17] ILIĆ,D.: *Swirl flow in a conical diffuser*, Ph.D. thesis, University of Belgrade, Faculty of Mechanical Engineering, Belgrade, 2013.

[18] ACRIVLELLIS,M., ČANTRAK,S., JUNGBLUTH,H.: *Statistical properties of turbulent swirl flow in pipes*, ZAMM, 1982, Band 62.

[19] PASHTRAPANSKA,M., JOVANOVIĆ,J., LIENHART,H., DURST,F.: *Turbulence measurements in a swirling pipe flow*, Experiments in Fluids, 2006, 41, pp.813-827.

[20] KITOH,O.: *Experimental study of turbulent swirling flow in a straight pipe*, Journal of Fluid Mechanics, 1991, 225, pp.445-479.

[21] BURAZER,J., LEČIĆ,M. ČANTRAK,S.: *On the non-local turbulent transport and non-gradient thermal diffusion phenomena in HVAC systems*, FME Transactions, 2012, 40, No.3, pp.119-125.

[22] RISTIĆ,S., ILIĆ,J., ČANTRAK,Đ., RISTIĆ,O., JANKOVIĆ,N.: *Estimation of laser-Doppler anemometry measuring volume displacement in cylindrical pipe flow*, Thermal Science, 2012, 16, No.4, pp.1127-1142.

[23] ILIĆ,J., RISTIĆ,S., ČANTRAK,Đ., JANKOVIĆ,N., SREĆKOVIĆ M.: *The comparison of air flow LDA measurement in simple cylindrical and cylindrical tube with flat external wall*, FME Transactions, 2013, Vol.41, No.4, pp.333-341.

[24] DURST,F., MELLING,A., WHITELAW,J.H.: *Principles and practice of laser-Doppler anemometry*, second edition, Academic Press, 1981.

[25] ČANTRAK,Đ., RISTIĆ,S., JANKOVIĆ,N.: *LDA, Classical probes and flow visualization in experimental investigation of turbulent swirl flow, DEMI 2011*, 10th International Conference on Accomplishments in Electrical and Mechanical Engineering and Information Technology, Banja Luka, Republika Srpska, 26-28 May 2011, Proceedings, pp.489-494.

Received: 09.09.2014.

Uticaj ugla lopatice aksijalnog ventilatora na karakteristike turbulentnog vihornog strujanja

U ovom radu je prikazano istraživanje turbulentnog vihornog strujanja u cevi na potisu aksijalnog ventilatora sa devet podesivih lopatica za uglove 22°, 26° i 30° i istovetni broj obrtaja (1500 min^{-1}). Brzine su merene laser Dopler anemometarskom tehnikom u mernom preseku 3.35·D od ulaska u instalaciju. Postignuti su Rejnoldsovi brojevi Re=236784, 259151 i 277018. Prikazana je nehomogenost i anizotropnost izučavanog turbulentnog brzinskog polja. Profili vremenski osrednjenih obimskih brzina imaju karakter Rankinovog vrtloga, dok se u slučaju aksijalnih brzina primećuje povratno strujanje u oblasti vrtložnog jezgra za uglove 26° i 30°. Eksperimentalno određeni momenti drugog i viših redova prikazuju kompleksnost turbulentnog vihornog strujanja. Vizualizacija turbulentnog vihornog strujanja je prikazana za ugao 22°.

Ključne reči: **aksijalni ventilator, turbulencija, vihorno strujanje, vizuelizacija strujanja, laser Dopler anemometrija.**

Влияние угла лопастей осевого вентилятора на характеристики турбулентного вихревого потока

Эта статья представляет исследование турбулентного потока в трубе для выполнения осевого вентилятора с девятью регулируемыми лопатками для углов 22°, 26° и 30° и одинаковое число оборотов (1500 min^{-1}). Скорости измеряются методом лазерной Допплеровской анемометрии в мерном пересечении 3:35 • D от входа в установку. Выполнены числа Рейнольдса Re = 236784, 259151 и 277018. Здесь показана неоднородность и анизотропия исследованого турбулентного скоростного поля. Профайлы усреднённых по времени окружных скоростей имеют характер вихря Ренкина, пока в случае осевых скоростей замечается обратный поток в области вихревого ядра для углов 26° и 30°. Экспериментально определённые моменты второго и более высоких порядков показывают сложность турбулентного вихревого потока. Визуализация турбулентного вихревого потока показана про угол 22°.

Ключевые слова: **осевой вентилятор, турбулентность, турбулентный вихревой поток, визуализация потока, лазерная Допплеровская анемометрия**.

Influence de l'angle de l'aube du ventilateur axial sur les caractéristiques du courant turbulent de tourbillon

Ce travail présente les recherches sur le courant turbulent de tourbillon dans la tube derrière le ventilateur axial à neuf aubes ajustables pour les angles de 22º, 26º et 30º et pour le même nombre de tours (1500 min'¹). Les vitesses ont été mesurées par la technique laser Doppler anémométrique dans la section de mesurage 3.35 · D à partir de son entrée dans l'installation . On a réalisé les suivantes nombres de Reynolds : Re = 236784, 259151 et 277018. On a présenté la non homogénéité et l'anisotropie du champ turbulent de vitesse étudié. Les profils des vitesses de moyen volume temporellement ont le caractère du vortex de Rankine alors que chez les vitesses axiales on peut observer le courant réversible dans le domaine du noyau de vortex pour les angles de 26º et 30º. Les moments déterminés par la voie expérimentale pour le second ordre et pour les ordres plus hauts révèlent toute la complexité du courent turbulent de tourbillon. La visualisation du courent turbulent de tourbillon a été présentée pour l'angle de 22º.

Mors clés: **ventilateur axial, turbulence, courant de tourbillon, visualisation de courant, anémométrie, laser Doppler**